Preprints of the 21st IFAC World Congress (Virtual)
Berlin, Germany, July 12-17, 2020

Fractional order [Proportional Integral Derivative] Controller Design with Specification Constraints: More Flat Phase Idea

Zhenlong Wu*, Yuquan Chen, Jairo Viola***, Ying Luo****, YangQuan Chen***, Donghai Li***

**State Key Lab of Power System, Department of Energy and Power Engineering, Tsinghua University, Beijing, 100084 China.*
***Department of Automation, University of Science and Technology of China, Hefei, 230026 China.*
**** Mechatronics, Embedded Systems and Automation (MESA) Lab, School of Engineering, University of California, Merced, CA 95343 USA. (Corresponding Author: **YangQuan Chen**; e-mail: ychen53@ucmerced.edu).*
***** School of Mechanical Science & Engineering, Huazhong University of Science and Technology, Wuhan, 430074 China.*

Abstract: The fractional order proportional integral derivative controller is attracting more and more attention. To design a controller with some specification constraints for the first order plus time delay (FOPTD) system, the idea of the "more flat phase" and the structure of the fractional order [proportional integral derivative] (FO[PID]) controller are proposed in this paper. Firstly, the stability region of the FO[PID] controller and the controller design with the "more flat phase" are introduced. Then the design procedure is presented by a simulation, and the pseudo code of the design procedure to obtain the parameter pairs and the achievable region is offered. The effectiveness of the proposed design method for the FO[PID] controller is verified by the experiment on the Peltier temperature control platform and the experiment results show a great potential in industrial applications.

Keywords: Fractional order [proportional integral derivative] controller, specification constraints, first order plus time delay system, more flat phase, the achievable region, Peltier temperature control platform.

1. INTRODUCTION

The fractional calculus has experienced an explosive growth in past decades. The fractional calculus is often used to model the various kinds of physical systems (Dumitru, 2012), such as perturbed pressurized heavy water reactor (Lamba et al. 2017) and lead-acid battery (Sabatier et al. 2010). The fractional order controllers based on the fractional calculus also have attracted many attentions such as fractional order proportional integral derivative (FOPID) controller (Shah et al. 2010), fractional order sliding mode controller (FOSMC) (Delavari et al. 2010), fractional order disturbance observer controller (FODOC) (Delavari et al. 2010) and fractional order active disturbance rejection control (FOADRC) (Li et al. 2010). FOPID, as the generalization of the classical integer order proportional integral derivative (IOPID) controller, has played a promising and indispensable role in industrial applications (Tepljakov et al. 2018).

The FOPID has five parameters to tune, which means the FOPID has more flexibility to obtain satisfactory control performance than the IOPID. However, more parameters means more difficulties in parameter tuning. To enhance the control performance and simplify the tuning procedure, many tuning methods have been proposed such as multi-objective optimization (Sánchez et al. 2017) and probabilistic robustness design (Wu et al. 2018). These tuning methods need huge computation and some of them lack the rigorous theoretical analysis. Some modified FOPIDs such as fuzzy FOPID (Moafi et al. 2016), adaptive FOPID (Arpaci et al. 2017) and Neural FOPID (Yaghi et al. 2019) are also proposed to enhance the control performance by combining advanced control theory, which result in the difficulty of the implementation on industrial control platforms.

Recently, a tuning method with specification constraints, a specified gain crossover frequency, a specified phase margin and the flat phase constraint, is proposed to design the robust fractional order proportional integral (FOPI) controller, fractional order [proportional integral] (FO[PI]) controller and fractional order [proportional derivative] (FO[PD]) controller (Luo et al. 2012; Luo et al. 2010; Luo et al. 2009). Based on the proposed tuning procedure, the fractional order controller can obtain better control performance than that of integer order controllers. The controller parameters can be decided solely with three specification constraints. If we want to extend the tuning method to the FOPID controller, it can be found that one has to tune five parameters with only three specification constraints. The parameters of the FOPID controller are not unique and how to select the appropriate parameters is another hard work.

As we all know, the flat phase constraint can ensure the open-loop phase is a constant around the given gain crossover frequency and this means the closed-loop system is not sensitive to the gain variation (Luo et al. 2012). To enhance the iso-damping property for the system response, the idea of "more flat phase" is proposed to tune the parameters of fractional order controller when the parameters number (n) is larger than three where the first order, second order …, $(n-2)th$ order derivative of the open-loop phase is applied. The more flat phase constraints means the more possible the open-loop phase is a constant and less sensitive to the gain variation for the closed-loop system. In this paper, the idea of

the "more flat phase" is applied to tune the fractional order proportional integral derivative (FO[PID]) controller which has four parameters. The main contributions of this paper are summarized as follows:

1) The idea of the "more flat phase" is proposed to design the FO[PID] controller.
2) The tuning procedure of the FO[PID] with "more flat phase" specification constraints is deduced and discussed.
3) The effectiveness of the proposed design synthesis is verified by the experiment based on the Peltier temperature control platform.

The rest of the paper is organized as follows. Section 2 formulates the design synthesis of the FO[PID] controller with "more flat phase" specification constraints for first order plus time delay (FOPTD) systems. In Section 3, the tuning procedure is summarized and a simulation is carried out to show the control performance of the FO[PID] controller. The experiment results are shown to verify the effectiveness of the proposed synthesis in Section4. Finally, Section 5 offers concluding remarks.

2. ROBUST FO[PID] CONTROLLER DESIGN FOR FOPTD SYSTEMS

2.1 The control structure

The control structure combining the controlled plant $P(s)$, the FO[PID] controller $C(s)$ and the gain-phase margin tester $M_T(A,\phi)$ (Chang et al. 1990) is shown in Fig. 1. $P(s)$ is a stable FOPTD system which can be depicted as,

$$P(s)=\frac{K}{Ts+1}e^{-Ls}, \tag{1}$$

where K, T and L are the gain, the time constant and the time delay of the controlled plant, respectively. The reason we choose a FOPTD system is that most industrial processes can be modelled as FOPTD systems by different model order reduction methods. The controller design method discussed in this paper will be extended for unstable and integrating systems in the future work.

The FO[PID] controller, $C(s)$, has the following type,

$$C(s)=\left(K_p+\frac{K_i}{s}+K_d s\right)^r, \tag{2}$$

where K_p, K_i, K_d and r are the proportional gain, integral gain, derivative gain and the order of the FO[PID] controller, respectively. r should locate in the range (0, 2).

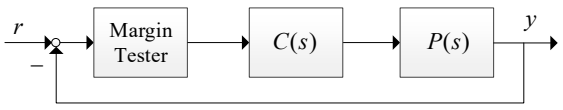

Fig. 1. The control structure with the margin tester.

The gain-phase margin tester, $M_T(A,\phi)$, is applied to calculate the parameter boundary of the controller with the specified gain margin and phase margin. Its transfer function is depicted by

$$M_T(A,\phi)=Ae^{-j\phi}, \tag{3}$$

where A and ϕ are the gain margin and phase margin, respectively. We can obtain the parameter boundaries with the given gain margin (phase margin) when we set $\phi=0$ ($A=1$).

2.2 The stability region of the FO[PID] controller

The open-loop of the control structure in Fig. 1 can be obtained as,

$$G_{op}(s)=M_T(A,\phi)C(s)P(s), \tag{4}$$

and the transfer function of the closed-loop system combining (1)-(3) is,

$$T_{cl}(s)=\frac{M_T(A,\phi)C(s)P(s)}{1+M_T(A,\phi)C(s)P(s)}$$

$$=\frac{Ae^{-j\phi}e^{-Ls}K\left(K_d s^2+K_p s+K_i\right)^r}{(Ts+1)s^r+Ae^{-j\phi}e^{-Ls}K\left(K_d s^2+K_p s+K_i\right)^r}. \tag{5}$$

Then we have the characteristic equation of the closed-loop system,

$$D\left(K_d,K_p,K_i,r,A,\phi;s\right)$$

$$=(Ts+1)s^r+Ae^{-j\phi}e^{-Ls}K\left(K_d s^2+K_p s+K_i\right)^r=0. \tag{6}$$

The parameter boundaries of K_p and K_i with the fixed K_d and r can be determined by two parts.

The first part is the real root boundary (RRB), which can be obtained by $D\left(K_d,K_p,K_i,r,A,\phi;s=0\right)=0$, and this means that the RRB is,

$$K_i^r=0. \tag{7}$$

The second part is the complex root boundary (CRB), which is obtained by $D\left(K_d,K_p,K_i,r,A,\phi;s=j\omega\right)$, and we have,

$$D\left(K_d,K_p,K_i,r,A,\phi;s=j\omega\right)$$

$$=(Tj\omega+1)(j\omega)^r+Ae^{-j\phi}e^{-Lj\omega}K\left(K_d(j\omega)^2+K_p j\omega+K_i\right)^r$$

$$=(jT\omega+1)\omega^r+AKR^r e^{j(r\theta-\omega L-\phi-r\pi/2)}=0, \tag{8}$$

where $j^r=e^{jr\pi/2}$, $R=\sqrt{\left(K_p\omega\right)^2+\left(K_i-K_d\omega^2\right)^2}$, and $\theta=\text{atan}\frac{K_p\omega}{K_i-K_d\omega^2}$, $\theta\in(-\pi,\pi)$.

We can obtain the real part and imaginary part based on (8),

$$\omega^r+AKR^r\cos E=0, \tag{9}$$

$$T\omega^{r+1}+AKR^r\sin E=0, \tag{10}$$

where we have,

$$R=\sqrt{\left(K_p\omega\right)^2+\left(K_i-K_d\omega^2\right)^2}, \tag{11}$$

and

$$E=r\theta-\omega L-\phi-r\pi/2\,. \tag{12}$$

Based on (9)-(12), we can obtain,

$$K_i=\begin{cases}\left|\sqrt{\dfrac{R^2}{1+(\tan\theta)^2}}\right|, \theta\in\left(-\dfrac{\pi}{2},\dfrac{\pi}{2}\right)\\ -\left|\sqrt{\dfrac{R^2}{1+(\tan\theta)^2}}\right|, \theta\in\left(-\pi,-\dfrac{\pi}{2}\right)\cup\left(\dfrac{\pi}{2},\pi\right)\end{cases}, \tag{13}$$

and

$$K_p=\begin{cases}\left|\dfrac{\left(K_i-K_d\omega^2\right)\tan\theta}{\omega}\right|, \theta\in(0,\pi)\\ -\left|\dfrac{\left(K_i-K_d\omega^2\right)\tan\theta}{\omega}\right|, \theta\in(-\pi,0)\end{cases}. \tag{14}$$

Now we can obtain the parameter pair $\{K_p,\ K_i\}$ boundary with the fixed r and K_d by sweeping over all ω from 0 to $+\infty$ (Luo et al. 2012). With all different r and K_d, we can obtain the complete stability region of the FO[PID] parameters.

2.3 The FO[PID] controller design with the "more flat phase"

If the number of design constraints is smaller than the number of fractional order controller parameters, n, the parameter pair is not the unique. The "more flat phase" is proposed to ensure the numbers of design constraints and controller parameters are the same and optimize the reasonable parameter regions. Specifically, the controller design constraints are the gain crossover frequency, the phase margin, the first order, derivative of the open-loop phase, …, $(n-2)th$ order derivative of the open-loop phase when the controller has n parameters. More flat phase constraints mean that the open-loop phase is more likely to be a constant and the closed-loop system is less sensitive to the gain variation.

By setting $A=1$ and $\phi=\phi_m$, where ϕ_m is the specified phase margin, we can obtain the parameter pair $\{K_p,\ K_i\}$ boundary by sweeping over ω from 0 to $\omega_{\max}$ with the fixed r and K_d. $\omega_{\max}$ is the maximum frequency on the relative stability region for the closed-loop system (Luo et al. 2012). Then we consider another constraint of the specified gain crossover frequency. Based on the characteristic equation in (6) and we have,

$$1+M_T(A,\phi)C(s)P(s)|_{s=j\omega}=0\,. \tag{15}$$

(15) can equal to the following expression,

$$G_{op}(s)_{s=j\omega}=M_T(A,\phi)C(s)P(s)|_{s=j\omega}=-1\,. \tag{16}$$

The magnitude equation based on (16) is,

$$\left|M_T(A,\phi)C(s)P(s)|_{s=j\omega}\right|=1\,, \tag{17}$$

and the phase equation is,

$$\angle\left(M_T(A,\phi)C(s)P(s)|_{s=j\omega}\right)=-\pi\,. \tag{18}$$

To satisfy the constraints of the flat phase and the "more flat phase", the derivative, …, $n-2$ order derivative of the open-loop phase should equal to zero. As discussed above, we have $\theta=\phi-\pi$ by setting $A=1$ and,

$$\begin{cases}\dfrac{d\phi}{d\omega}=0\\ \cdots\\ \dfrac{d^{(n-2)}\theta}{d\omega^{(n-2)}}=\dfrac{d^{(n-2)}\phi}{d\omega^{(n-2)}}=0\end{cases}. \tag{19}$$

For the FO[PID] controller, we have,

$$\frac{d\phi}{d\omega}=\frac{rK_p\left(K_i+K_d\omega^2\right)}{\left(K_p\omega\right)^2+\left(K_i-K_d\omega^2\right)^2}-L-\frac{T}{1+(T\omega)^2}=0\,, \tag{20}$$

and

$$\frac{d^2\phi}{d\omega^2}=2rK_p\frac{K_d\omega\left[\left(K_p\omega\right)^2+\left(K_i-K_d\omega^2\right)^2\right]}{\left[\left(K_p\omega\right)^2+\left(K_i-K_d\omega^2\right)^2\right]^2}$$
$$-2rK_p\frac{\left(K_i+K_d\omega^2\right)\left[K_p^2\omega-2K_d\omega\left(K_i-K_d\omega^2\right)\right]}{\left[\left(K_p\omega\right)^2+\left(K_i-K_d\omega^2\right)^2\right]^2}+\frac{2T^3\omega}{\left[1+(T\omega)^2\right]^2}$$
$$=0\,. \tag{21}$$

Thus, the FO[PID] controller parameters can be decided by the gain crossover frequency, phase margin, flat phase, second order derivative of the open-loop phase. Based on equations (20) and (21), the idea of "more flat phase" can be applied to the FO[PID] controller and FO[PID] controller designed with the "more flat phase" idea can be used to verify the superiority of the "more flat phase" idea. That is the reason that we discuss the design of the FO[PID] controller in this paper.

Besides, we can obtain the achievable region by sweeping over the phase margin $\phi_m\in(0,\pi)$ and the gain crossover frequency $\omega\in(0,\omega_{\max}]$ (Luo et al. 2012). All possible constraint pair $\{\phi_m,\ \omega\}$ in the achievable region can be checked before the controller design and the achievable region offers us a reasonable design constraint pair $\{\phi_m,\ \omega\}$.

3. DESING PROCEDURE AND SIMULATIONS

Based on the discussions in Section 2, the design procedure is presented. Besides, the pseudo code and simulation results are also given.

Step 1: give a stable FOPTD system with $K=1$, T=1 and L=0.1 with two specifications, a specified phase margin, ϕ_m=78° , and a specified gain crossover frequency, ω_{gc}=4 rad / s .

Step 2: Choose a fixed r and K_d, and we can obtain the CRB by setting $A=1$ and $\phi=\phi_m$ as shown in Fig. 2. By

sweeping over all $K_d \in (-T/AK, T/AK)$, we can obtain all CRB with the different ϕ_m, as shown in Fig. 3. Note that the range of K_d is given as $(-T/AK, T/AK)$ (Luo et al. 2012).

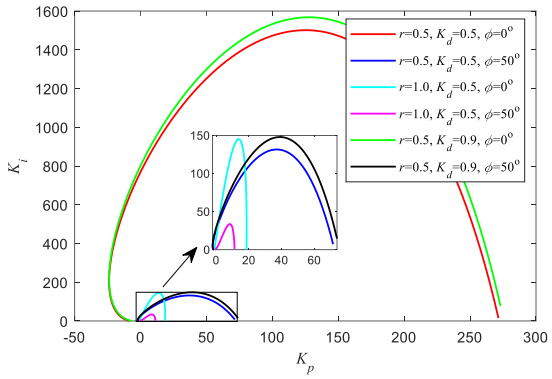

Fig. 2. The CRB with different r, K_d and $\phi = \phi_m$.

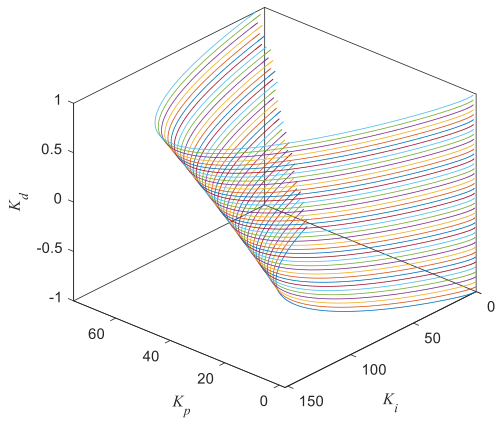

Fig. 3. The CRB by sweeping over $K_d \in (-1,1)$ with the fixed $r = 0.5$.

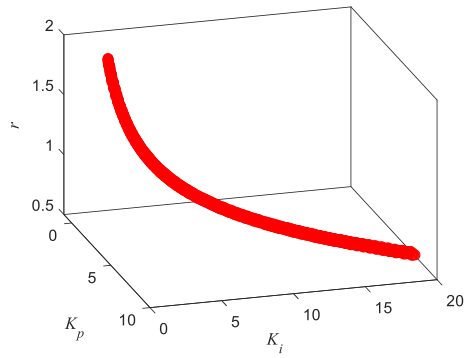

Fig. 4. The parameter band satisfied the specified ω_{gc}, the specified ϕ_m and the flat phase.

Step 3: With the chosen ϕ_m=78° and ω_{gc}=4 rad/s, we can obtain a parameter band with the parameter pair $\{K_p, K_i, r\}$ by satisfying the constants of the specified ω_{gc}, the specified ϕ_m and the flat phase. Note that the parameter pair $\{K_p, K_i, r\}$ is a parameter band as shown in Fig. 4 while the parameter pair $\{K_p, K_i, r\}$ of the FOPI controller is a curve as discussed in (Luo et al. 2012). Besides, we can also obtain the parameter band with the parameter pair $\{K_p, K_i, r\}$ by satisfying the constants of the specified ω_{gc}, the specified ϕ_m and the second order derivative of the open loop phase (which also equals to the derivative of the flat phase) as shown in Fig. 5.

Step 4: Based on these two parameter bands, we can obtain the intersection of the two parameter bands as shown in Fig. 6. All parameter pairs $\{K_p, K_i, r\}$ in the intersection satisfy the four control constraints, the specified phase margin, the specified gain crossover frequency, the flat phase and the derivative of flat phase in (19).

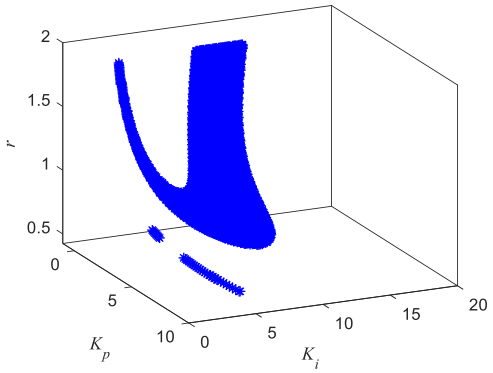

Fig. 5. The parameter band satisfied the specified ω_{gc}, the specified ϕ_m and the second order derivative of the open loop phase.

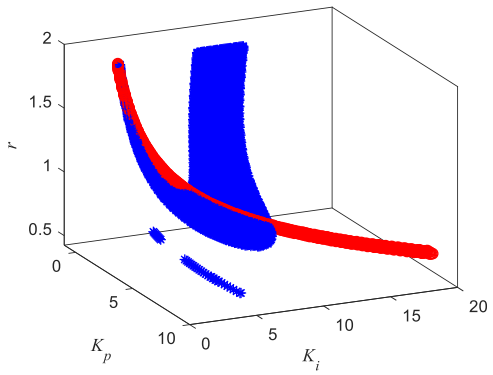

Fig. 6. The intersection of the two parameter bands (*: *The parameter band satisfied the specified ω_{gc}, the specified ϕ_m and the flat phase; o: The parameter band satisfied the specified ω_{gc}, the specified ϕ_m and the second order derivative of the open loop phase*).

Step 5: Select any parameter pair in the intersection as the parameters of the FO[PID] controller. Then we can obtain the responses of the closed-loop system in time-domain and frequency-domain. As shown in Fig. 7, we select two parameter pairs $\{K_p = 4.6170, K_i = 6.9277, K_d = 0.3650, r = 0.9250\}$ and $\{K_p = 2.1816, K_i = 1.7017, K_d = 0.0900,$

$r=1.8150$ } randomly to test the control performance. Fig. 8 and Fig. 9 are the responses in time-domain and frequency-domain of the selected parameter pair 1, responsively, where the loop gain is set to be 80%, 100% and 120% of the nominal value. Besides, the responses in time-domain of the selected parameter pair 2 is shown in Fig. 10 where the loop gain is also set to be 80%, 100% and 120% of the nominal value. Besides, the responses in frequency-domain of the selected parameter pair 2 are also shown in Fig. 8. We can know that the closed-loop system is not sensitive to the variation of the loop gain and the closed-loop system can obtain the satisfactory control performance with the proposed design method.

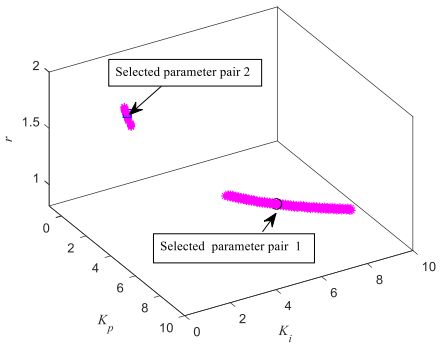

Fig. 7. The selected parameter pairs from the intersection.

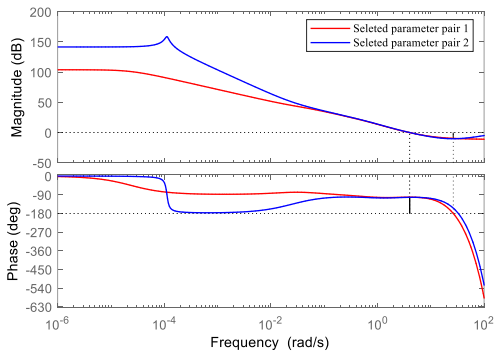

Fig. 8. The open-loop frequency response of the selected parameter pairs.

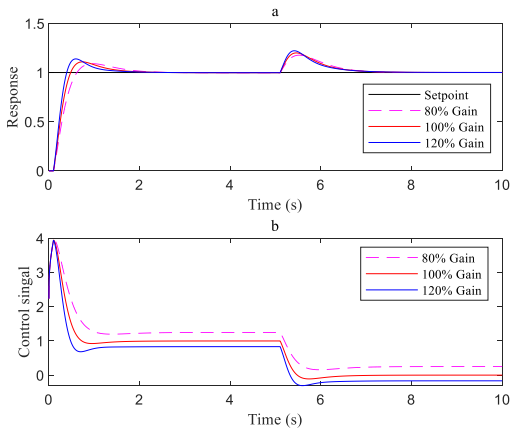

Fig. 9. The control performance with the selected parameter pair 1. (*a: the output response; b: the control signal*)

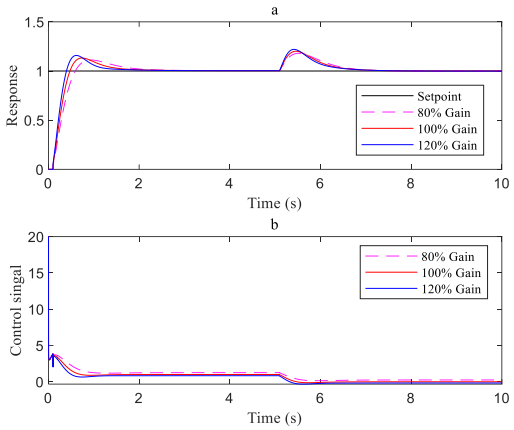

Fig. 10. The control performance with the selected parameter pair 2. (*a: the output response; b: the control signal*)

Remark 1: To explain the effectiveness of the design method, another two specifications are set as ϕ_m=83° and ω_{gc}=4 rad / s . Then we can obtain the intersection satisfying the four control constraints as shown in Fig. 11. We select one parameter pair { $K_p=4.7401$, $K_i=6.3553$, $K_d=0.4400$, $r=0.9100$ } to test the control performance and the results are shown in Fig. 12. We can know that the closed-loop system is not sensitive to the variation of the loop gain and the overshoots in Fig. 12 are smaller than that in Fig. 9 and Fig. 10.

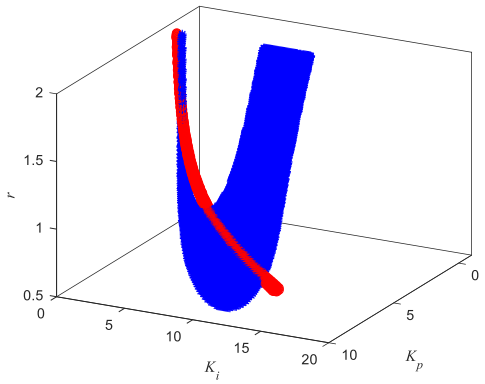

Fig. 11. The intersection of the two parameter bands. (**: The parameter band satisfied the specified ω_{gc}, the specified ϕ_m and the flat phase; o: The parameter band satisfied the specified ω_{gc}, the specified ϕ_m and the derivative of flat phase.*)

Step 6: By sweeping over all phase margin, $\phi_m \in (0,180^\circ)$, and a specified gain crossover frequency, $\omega_{gc} \in (0,20)$, we can obtain the achievable region { ϕ_m , ω_{gc} } of the FO[PID] controller as shown in Fig. 13.

Remark 2: To compare the control performance between the IOPID and FO[PID] controllers, the IOPID parameter pair with specification constraints { ω_{gc}=4 rad / s , ϕ_m=83° , $d\phi/d\omega$=0 } is obtained as { $K_p=4.1209$, $K_i=4.8983$,

$K_d = 0.3400$ }. The control performance of the IOPID controller with uncertain gains is presented in Fig. 14. It can be learnt that the overshoot of the closed-loop system has an obvious increase with the increasing of the gain K. Generally, the proposed design method with "more flat phase" idea is not sensitive to the variation of the loop gain and can obtain the satisfactory control specifications.

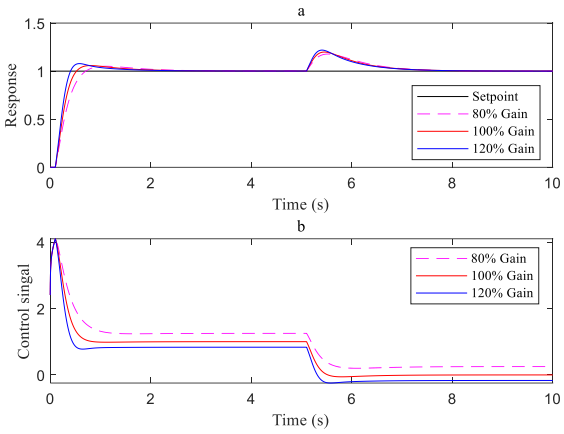

Fig. 12. The control performance with the parameter pair satisfying ϕ_m=83° and ω_{gc}=4 rad / s .

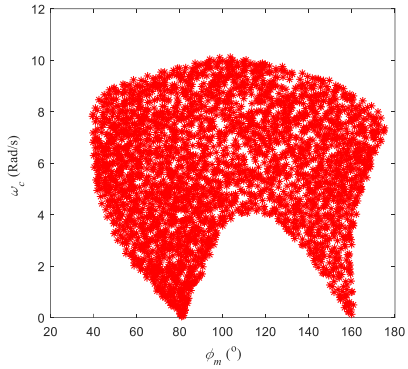

Fig. 13. The achievable region of the FO[PID] controller.

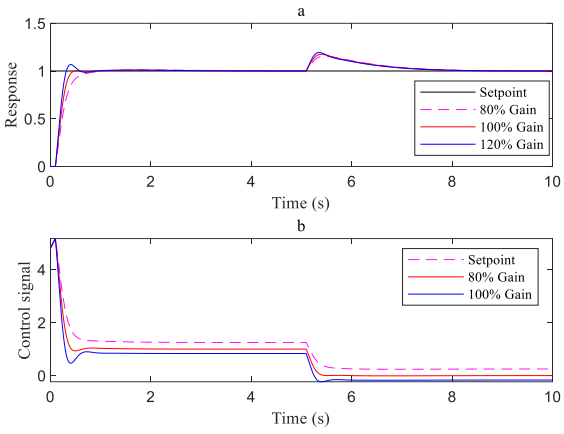

Fig. 14. The control performance of the IOPID controller with the parameter pair satisfying ϕ_m=83° and ω_{gc}=4 rad / s .

Generally, the "more flat phase" idea can guarantee the more possible the open-loop phase is a constant and less sensitive to the gain variation for the closed-loop system with satisfactory control performance. That is why the FO[PID] controller is superior to the IOPID controller as discussed above.

Remark 3: To obtain the response of the closed-loop system in time-domain, the approximation to implement the FO[PID] controller in MATLAB or SIMULINK is necessary and this is bound to bring some approximation error. In this paper, the frequency-domain response of the FO[PID] is fitted by a fourth-order rational transfer function and the transfer function is applied in all simulations and experiments. Based on the results of comparative tests, it can be learnt that the approximation error is small and can be used to obtain the time-domain response.

4. EXPERIMENTAL VERIFICATION

Based on the confidence built in the theoretical analysis and simulation results, the FO[PID] controller with the proposed design method is applied to the Peltier temperature control platform in this section. The platform is built with Peltier (thermo electronic) modules and thermo sensors as shown in Fig. 15. The controlled variable and the control signal for the Peltier temperature control platform are the output temperature and the voltage, respectively. The voltage value is the bi-directional PWM signal having a resolution of 2^8 for 9V, representing 0 % ~ 100 % duty cycle. Note that a delay element and a gain regulator k_{gc} are added before the control signal is sent to the Peltier modules. The goal is to build a FOPTD system and adjust the loop gain by setting different k_{gc}. The nominal value of k_{gc} is one, and then is set as 0.8 and 1.2 to reflect the variation of the loop gain.

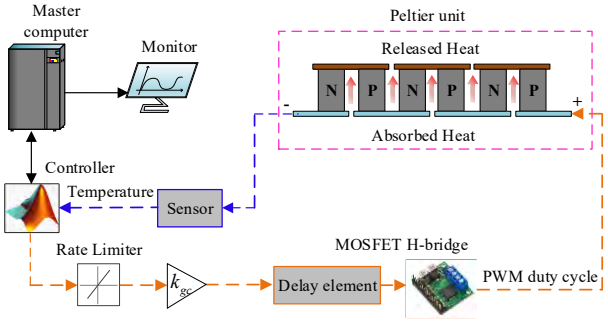

Fig. 15. The control structure of the Peltier temperature control platform.

With the identified model of the system, the parameters of the FO[PID] controller can be obtained as { $K_p = 5.121$, $K_i = 0.041$, $K_d = 1.010$, $r = 1.202$ } using the proposed tuning method and the FO[PID] controller is applied to the Peltier temperature control platform. The experiment results are presented in Fig. 16, where the input disturbance has step changes at 600s (with an amplitude of negative 50) and 1600s (with an amplitude of positive 50), respectively. We can know that the closed-loop system with the designed FO[PID] controller is not sensitive to the variation of the loop gain and the closed-loop system can obtain the satisfactory control performance when the loop gain has variations. Moreover, the time constant of the Peltier temperature system

also has a slight deviation with the change of the gain regulator. The changing controlled plants with the FO[PID] controller result in the deviation of the disturbance rejection abilities as shown in Fig. 16.

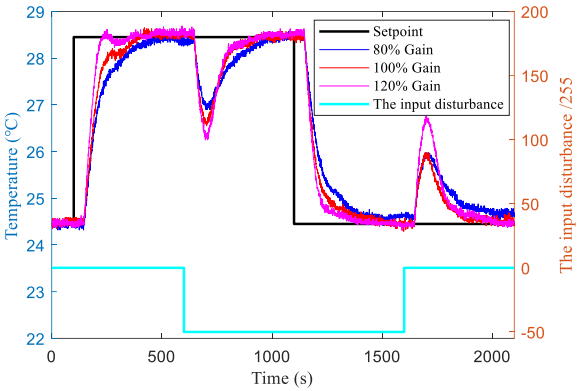

Fig. 16. The experiment results with the setpoint step and the input disturbance.

5. CONCLUSIONS

The idea of the "more flat phase" is proposed to tune the parameters of fractional order controller when there are more than three parameters in this paper and the idea is applied to design FO[PID] controller which has four parameters. The stability region of the FO[PID] controller, the design procedure and the pseudo code to obtain the achievable region are discussed. Besides, the effectiveness of the proposed design method for the FO[PID] controller is verified by a simulation and an experiment on the Peltier temperature control platform. The simulation and experimental results show that the FO[PID] controller designed with the "more flat phase" is not sensitive to the variation of the loop gain and can obtain the satisfied control specifications. The idea of the "more flat phase" shows a great potential in the fractional controller design which has more than three parameters. In the future work, the "more flat phase" will be extended for unstable and integrating systems and the procedure should be compared with the standard robust control procedure yielding a low-dimension controller.

ACKNOWLEDGEMENT

The first author would like to give thanks to the China Scholarship Council (CSC), Grant 201806210219, for funding towards research at University of California, Merced, from Sep. 2018 to Sep. 2019.

REFERENCES

Arpaci, H., and Ozguven, O.F. (2017). Design of adaptive fractional-order PID controller to enhance robustness by means of adaptive network fuzzy inference system. *International Journal of Fuzzy Systems,* volume (19), 1118-1131.

Chang, C. H., and Han, K. W. (1990). Gain margins and phase margins for control systems with adjustable parameters. *Journal of Guidance, Control, and Dynamics,* volume (13), 404–408.

Chen, Y.Q., Vinagre, B. M., and Podlubny I. (2004). Fractional order disturbance observer for robust vibration suppression. *Nonlinear Dynamics,* volume (38), 355-367.

Delavari, H., Ghaderi, R., Ranjbar, A., et al. (2010). Fuzzy fractional order sliding mode controller for nonlinear systems. *Communications in Nonlinear Science and Numerical Simulation,* volume (15), 963-978.

Dumitru, B., Kai, D., and Enrico S. (2012), *Fractional calculus: models and numerical methods*. World Scientific, Singapore.

Lamba, R., Singla, S. K., and Sondhi, S. (2017). Fractional order PID controller for power control in perturbed pressurized heavy water reactor. *Nuclear Engineering and Design*, volume (323), 84-94.

Li, D. Z., Ding, P., and Gao, Z. (2016). Fractional active disturbance rejection control. *ISA Transactions,* volume (62), 109-119.

Luo, Y., Chen, Y.Q., Wang, C.Y., et al. (2010). Tuning fractional order proportional integral controllers for fractional order systems. *Journal of Process Control,* volume (20), 823-831

Luo, Y., and Chen, Y.Q. (2009). Fractional order [proportional derivative] controller for a class of fractional order systems. *Automatica*, volume (45), 2446-2450.

Luo, Y., and Chen, Y.Q. (2012). Stabilizing and robust fractional order PI controller synthesis for first order plus time delay systems. *Automatica,* volume (48), 2159-2167.

Moafi, M., Marzband, M., Savaghebi, M., et al. (2016), Energy management system based on fuzzy fractional order PID controller for transient stability improvement in microgrids with energy storage. *International Transactions on Electrical Energy Systems,* volume (26), 2087-2106.

Sabatier, J., Cugnet, M., Laruelle, S., et al. (2010). A fractional order model for lead-acid battery crankability estimation. *Communications in Nonlinear Science and Numerical Simulation,* volume (15), 1308-1317.

Sánchez, H.S., Padula, F., Visioli, A., et al. (2017). Tuning rules for robust FOPID controllers based on multi-objective optimization with FOPDT models. *ISA Transactions,* volume (66), 344-361.

Shah, P., and Agashe, S. (2016). Review of fractional PID controller. *Mechatronics,* volume (38), 29-41.

Tepljakov, A., Alagoz, B.B., Yeroglu, C, et al. (2018). FOPID controllers and their industrial applications: A survey of recent results. *IFAC-PapersOnLine,* volume (51), 25-30.

Wu, Z. L., Li, D. H., Xue, Y. L., et al. (2018). Tuning for fractional order PID controller based on probabilistic robustness. *IFAC-PapersOnLine,* volume (51), 675-680.

Yaghi, M. A., and Efe, M.O. (2019), H2/H∞-Neural Based FOPID Controller Applied for Radar Guided Missile. *IEEE Transactions on Industrial Electronics.* (Early Access, DOI: 10.1109/TIE.2019.2927196).